Robust beamformer based on total variation minimisation and sparse-constraint

Y. Liu and Q. Wan

A sparse beam pattern constraint could suppress the sidelobe of the minimum variance distortionless response beamformer. But the array gains of the practical beam pattern are not in standard sparse distribution but dense in the mainlobe and sparse in the sidelobes. To improve performance, while revising the sparse constraint only on the sidelobe, a total variation minimisation of the whole beam pattern is incorporated to encourage large array gains accumulated in the mainlobe and small trivial array gains gathered in the sidelobes. Simulations demonstrate that performance enhancement is considerable for its lower sidelobe level and deeper nulling for interference, while robustness against the steering angle mismatch is maintained.

Introduction: The minimum variance distortionless response (MVDR) beamformer is a popular spatial signal processor used in sensor arrays to control the directionality of the reception or transmission of a signal. It has wide practical applications in wireless systems [1]. Compared to conventional beamformers, it has superior performance in interference-plus-noise suppression. However it can also present unacceptably high sidelobes, which would lead to serious performance reduction in the presence of high noise or unexpected interferences [2].

Recently a sparse array gain constraint was proposed to incorporate in the MVDR beamformer to enable sidelobe suppression [3]. For all the array gains in the beam pattern, the l_1 norm-based sparse constraint was added equally. However, the practical beam pattern has only sparse array gains in the sidelobes, and the array gains in the mainlobe are distributed as a solid block. To enhance the performance further by better fitting the practical array gains, the l_1 norm-based sparse array gains constraint is added only to the sidelobes and a total variation minimisation of the array gains constraint restricts the whole beam pattern. Numerical evaluations show that the proposed beamformer achieves a better performance.

Signal model: The signal impinging onto a uniform linear array (ULA) with M antennas can be represented by an M-by-1 vector:

$$\boldsymbol{x}(k) = s(k)\boldsymbol{a}(\theta_0) + \sum_{j=1}^{J} \beta_j(k)\boldsymbol{a}(\theta_j) + \boldsymbol{n}(k) \tag{1}$$

where k is the index of time, J is the number of interference sources, $s(k)$ and $\beta_j(k)$ (for $j = 1, \ldots, J$) are the amplitudes of the signal of interest (SOI) and interfering signals at time instant k, respectively, θ_l (for $l = 0, 1, \ldots, J$) are the direction of arrivals (DOAs) of the SOI and interfering signals, $\boldsymbol{a}(\theta_l) = [1\ \exp(j\,\varphi_l) \ldots \exp(j(M-1)\,\varphi_l)]^T$ (for $l = 0, 1, \ldots, J$) are the steering vectors of the SOI and interfering signals, wherein $\varphi_l = (2\pi d/\lambda)\sin\theta_l$, with d being the distance between two adjacent sensors and λ being the wavelength of the SOI; and $\boldsymbol{n}(k)$ is the additive white Gaussian noise (AWGN) vector at time instant k.

The output of a beamformer for the time instant k is then given by

$$y(k) = \boldsymbol{w}^H\boldsymbol{x}(k) = s(k)\boldsymbol{w}^H\boldsymbol{a}(\theta_0) + \sum_{j=1}^{J} \beta_j(k)\boldsymbol{w}^H\boldsymbol{a}(\theta_j) + \boldsymbol{w}^H\boldsymbol{n}(k) \tag{2}$$

where $\boldsymbol{w}$ is the M-by-1 complex-valued weighting vector.

Proposed beamformer: The MVDR beamformer is desiged to minimise the total array output energy subject to a distortionless constraint in the DOA of the SOI [1]:

$$\boldsymbol{w}_{MVDR} = \arg\min_{\boldsymbol{w}} (\boldsymbol{w}^H\boldsymbol{R}_x\boldsymbol{w}),\ \text{s.t. } \boldsymbol{w}^H\boldsymbol{a}(\alpha_0) = 1 \tag{3}$$

where $\boldsymbol{R}_x$ is the M-by-M covariance matrix of the received signal vector $\boldsymbol{x}(k)$, and $\boldsymbol{w}^H\boldsymbol{a}(\alpha_0) = 1$ is the distortionless constraint applied to the SOI, with α_0 being the given DOA of the SOI, which may not be the same as θ_0 due to estimation error.

To reduce the sidelobe level of the MVDR beamformer, a sparse array gains constraint was incorporated in [3]:

$$\boldsymbol{w}_S = \arg\min_{\boldsymbol{w}} (\boldsymbol{w}^H\boldsymbol{R}_x\boldsymbol{w} + \gamma_1\|\boldsymbol{w}^H\boldsymbol{A}\|_1),\ \text{s.t. } \boldsymbol{w}^H\boldsymbol{a}(\alpha_0) = 1 \tag{4}$$

where γ_1 is the weighting parameter balancing the minimum variance constraint on the total array output energy and the sparse constraint on the beam pattern. The M- by- N $\boldsymbol{A}$ is the array manifold with α_n ($n = 1, 2, \ldots, N$) being the sampled angles in the range $[-90^\circ, 90^\circ]$, and the N steering vectors cover all the DOAs in the sampling range, i.e.

$$A_{mn} = \exp(j(m-1)\varphi_n), \quad \text{for } m = 1, \ldots, M,\ n = 1, \ldots, N \tag{5}$$

$$\varphi_n = \frac{2\pi d}{\lambda}\sin\alpha_n, \quad \text{for } n = 1, 2, \ldots, N \tag{6}$$

and $\|\boldsymbol{x}\|_1 = \sum|x_i|$ is the l_1 norm of a vector $\boldsymbol{x}$. It is a kind of measurement of sparsity for $\boldsymbol{x}$. The smaller the value of $\|\boldsymbol{x}\|_1$ is, the larger the number of trivial entries in $\boldsymbol{x}$ is [4]. The optimal weighting vector indicated by (4) can be solved in an iterative way efficiently [3].

The sparse constraint encourages sparse distribution for all the array gains $\boldsymbol{w}^H\boldsymbol{A}$ for all the possible DOAs from -90° to 90°. However, the array gains in the mainlobe are not sparse. On the contrary, the distribution of the entries of the beam pattern is dense as a solid block. Thus the performance would be improved by a more suitable constraint on the beam pattern. Here the l_1 norm minimisation-based sparse constraint is added only to the sidelobes, and a total variation minimisation (TVM) restricts the entire beam pattern [5]. The TVM and sparse-constraint-based MVDR (TVMS-MVDR) beamformer can be formulated as:

$$\boldsymbol{w}_{TVMS} = \arg\min_{\boldsymbol{w}}\Bigg(\boldsymbol{w}^H\boldsymbol{R}_x\boldsymbol{w} + \gamma_2\Bigg(\sum_{i=1}^{I}\|\boldsymbol{D}_i(\boldsymbol{w}^H\boldsymbol{A})^T\|_2 + \|\boldsymbol{w}^H\boldsymbol{A}_S\|_1\Bigg)\Bigg),\ \text{s.t. } \boldsymbol{w}^H\mathbf{a}(\alpha_0) = 1 \tag{7}$$

where

$$\boldsymbol{D}_i = \begin{bmatrix} \boldsymbol{D}_{i,F} \\ \boldsymbol{D}_{i,B} \end{bmatrix} \tag{8}$$

$$\boldsymbol{A}_S = [\,\boldsymbol{a}(\alpha_{-90}) \quad \ldots \quad \boldsymbol{a}(\alpha_{-b-1}) \quad \boldsymbol{a}(\alpha_{+b+1}) \quad \ldots \quad \boldsymbol{a}(\alpha_{+90})\,] \tag{9}$$

$\boldsymbol{D}_{i,F}$ and $\boldsymbol{D}_{i,B}$ are the ith forward and backward differential matrix, I is the total number of differential matrix $\boldsymbol{D}_i$ used in the model; $\boldsymbol{A}_S$ is constituted by the sidelobe steering vectors in $\boldsymbol{A}$. The product $\boldsymbol{w}^H\boldsymbol{A}_S$ indicates array gains of the sidelobe. γ_2 is the weighting factor controlling the TVM constraint and the sparse constraint; and b is an integer corresponding to the bounds between the mainlobe and the sidelobe of the beam pattern. Since the objective function of the proposed beamformer (7) is convex, the optimal $\boldsymbol{w}_{TVMS}$ can also be solved out by convex programming software CVX [6].

In the beam pattern shaping constraint $\sum_{i=1}^{I}\|\boldsymbol{D}_i(\boldsymbol{w}^H\boldsymbol{A})^T\|_2 + \|\boldsymbol{w}^H\boldsymbol{A}_S\|_1$, the first term is the TVM, which discourages the large fluctuation in the beam pattern. It results in the high array gains accumulated in the mainlobe and the small trivial ones gathered in the sidelobe. In addition, the sparse beam pattern constraint is modified to be the second term to suppress the sidelobe levels. As the new further constraint in (7) fits the desired beam pattern better, the performance would be enhanced.

Simulation: As the above methods have no particular requirement for the array structure [1, 3], in the simulations, a ULA with eight half-wavelength-spaced sensors is considered. The AWGN at each sensor is assumed spatially uncorrelated. The DOA of the SOI is set to be 0°, and the DOAs of three interfering signals are set to be -30°, 30° and 70°, respectively. The signal-to-noise ratio (SNR) is set to be 10 dB, and the interference-to-noise ratios (INRs) are assumed to be 20, 20 and 40 dB at -30°, 30°, and 70°, respectively. 100 snapshots are used for each simulation. The bounds parameter b is set to be 20, and γ_1, γ_2 are set to be 5. The matrix $\boldsymbol{A}$ consists of all steering vectors in the DOA range of $[-90^\circ, 90^\circ]$ with the sampling interval of 1°. The parameter for TVM in (7) is set to be $I = 2$.

To evaluate the performance in detail, the signal-to-interference-plus-noise ratio (SINR) is calculated via the following formula:

$$SINR = \frac{\sigma_S^2\boldsymbol{w}^H\boldsymbol{a}(\theta_0)\boldsymbol{a}^H(\theta_0)\boldsymbol{w}}{\boldsymbol{w}^H\left(\sum_{j=1}^{J}\sigma_j^2\boldsymbol{a}(\theta_j)\boldsymbol{a}^H(\theta_j) + \boldsymbol{Q}\right)\boldsymbol{w}} \tag{10}$$

where σ_S^2 and σ_j^2 are the variances of the SOI and jth interference, $\boldsymbol{Q}$ is a diagonal matrix with the diagonal elements being the noise variances.

Fig. 1 shows the normalised beam patterns of the MVDR beamformer (3), the sparse MVDR beamformer (4), and the proposed TVMS-MVDR beamformer (7) of 1000 Monte Carlo simulations. It is

obvious that the best sidelobe suppression performance is achieved by the TVMS-MVDR beamformer (7). Among the three beamformers, the TVMS-MVDR beamformer (7) has the lowest array gain level in the sidelobe area, and provides the deepest nulls in the directions of interference, i.e. -30°, 30° and 70°. The average received SINR by the beamformers defined in (3), (4) and (7) are 2.0732, 4.3178 and 5.8563 dB.

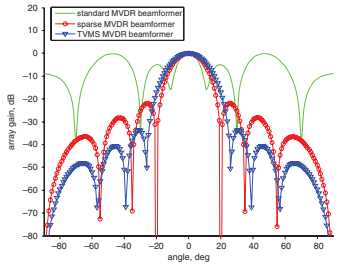

Fig. 1 *Normalised beam patterns of three beamformers without angle mismatch*

Fig. 2 shows the normalised beam patterns of the beamformers with each one having a 4° mismatch between the steering angle and the DOA of the SOI. We can see that the MVDR beamformer has a deep notch at 4°, which is the DOA of the SOI. Comparing the beam patterns of beamformers defined in (4) and (7), we can see that the TVMS-MVDR beamformer (7) further suppresses sidelobe levels and deepens the nulls for interference avoidance, and has almost the same robustness against mismatch. Although the TVMS-MVDR beamformer's main beam is slightly broader than that of the sparse MVDR beamformer, the much lower sidelobes and much deeper nullings for interferences obtained using the proposed method will mitigate this effect and the whole output SINR will be improved. In the case of 4° mismatch, the average received SINR by the beamformers defined in (3), (4) and (7) are 0.0004, 3.1903 and 4.8667 dB, respectively.

Simulations with different arrays, such as $M = 12$ and/or $M = 16$, 80 and/or 120 snapshots, etc., have also been performed. The performance gains can be obtained similarly.

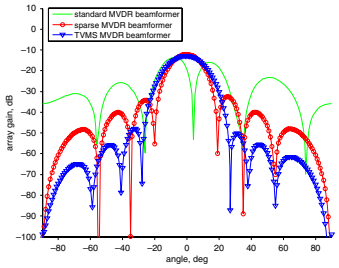

Fig. 2 *Normalised beam patterns of three beamformers with 4° angle mismatch*

Conclusion: The proposed TVMS-MVDR beamformer shows superiority to the MVDR beamformer and the sparse MVDR beamformer. It outperforms in terms of sidelobe suppression and nulling for interference avoidance, while maintaining robustness against DOA mismatch.

28 September 2010
doi: 10.1049/el.2010.8730
One or more of the Figures in this Letter are available in colour online.

Y. Liu and Q. Wan (*Department of Electronic Engineering, University of Electronic Science and Technology of China, Chengdu, 611731, People's Republic of China*)

E-mail: liuyipeng@uestc.edu.cn

References

1 Li, J., and Stoica, P.: 'Robust adaptive beamforming' (Wiley and Sons, New York, 2006)
2 Wax, M., and Anu, Y.: 'Performance analysis of the minimum variance beamformer', *IEEE Trans. Signal Process.*, 1996, **44**, (4), pp. 928–937
3 Zhang, Y., Ng, B.P., and Wan, Q.: 'Sidelobe suppression for adaptive beamforming with sparse constraint on beam pattern', *Electron. Lett.*, 2008, **44**, (10), pp. 615–616
4 Candes, E.J., and Wakin, M.B.: 'An introduction to compressive sampling', *IEEE Signal Process. Mag.*, 2008, **25**, (2), pp. 21–30
5 Yang, J., Zhang, Y., and Yin, W.: 'A fast alternating direction method for TVL1-L2 signal reconstruction from partial Fouire data', *IEEE J. Sel. Top. Signal Process.*, 2010, **4**, (2), pp. 288–297
6 Grant, M., Boyd, S., and Ye, Y.: 'CVX user' guide for CVX version 1.1', ([online accessible]: http://www.stanford.edu/~boyd/index.html)